Diabetologia (2020) 63:811–824
https://doi.org/10.1007/s00125-020-05090-y

ARTICLE

Obesity-induced reduced expression of the lncRNA ROIT impairs insulin transcription by downregulation of *Nkx6.1* methylation

Fang Fang Zhang[1] · Yu Hong Liu[1] · Dan Wei Wang[1] · Ting Sheng Liu[1] · Yue Yang[1] · Jia Min Guo[1] · Yi Pan[1] · Yan Feng Zhang[1] · Hong Du[2] · Ling Li[3] · Liang Jin[1]

Received: 13 June 2019 / Accepted: 9 December 2019 / Published online: 1 February 2020

Abstract

Aims/hypothesis Although obesity is a predisposing factor for pancreatic beta cell dysfunction, the mechanisms underlying its negative effect on insulin-secreting cells is still poorly understood. The aim of this study was to identify islet long non-coding RNAs (lncRNAs) involved in obesity-mediated beta cell dysfunction.

Methods RNA sequencing was performed to analyse the islets of high-fat diet (HFD)-fed mice and those of normal chow-fed mice (NCD). The function in beta cells of the selected lncRNA 1810019D21Rik (referred to in this paper as ROIT [regulator of insulin transcription]) was assessed after its overexpression or knockdown in MIN6 cells and primary islet cells, as well as in siRNA-treated mice. Then, RNA pull-down, RNA immunoprecipitation, coimmunoprecipitation and bisulphite sequencing were performed to investigate the mechanism of ROIT regulation of islet function.

Results ROIT was dramatically downregulated in the islets of the obese mice, as well as in the sera of obese donors with type 2 diabetes, and was suppressed by HNF1B. Overexpression of ROIT in MIN6 cells and islets led to improved glucose homeostasis and insulin transcription. Investigation of the mechanism involved showed that ROIT bound to DNA methyltransferase 3a and caused its degradation through the ubiquitin proteasome pathway, which blocked the methylation of the *Nkx6.1* promoter.

Conclusions/interpretation These findings functionally suggest a novel link between obesity and beta cell dysfunction via ROIT. Elucidating a precise mechanism for the effect of obesity on lncRNA expression will broaden our understanding of the pathophysiological development of diabetes and facilitate the design of better tools for diabetes prevention and treatment.

Data availability The raw RNA sequencing data are available from the NCBI Gene Expression Omnibus (GEO series accession number GSE139991).

Keywords DNA methyltransferase · DNMT3A · LncRNA · Nkx6.1 · Obesity · ROIT

Abbreviations

ChIP	Chromatin immunoprecipitation
CHX	Cyclohexamide
DAC	Decitabine
DMR	Differentially methylated region
DNMT	DNA methyltransferase
EMSA	Electrophoretic mobility shift assay
GAPDH	Glyceraldehyde-3-phosphate dehydrogenase
GSIS	Glucose-stimulated insulin secretion
HFD	High-fat diet
HNF1B	HNF1 homeobox B
LncRNA	Long non-coding RNA
NCD	Normal chow diet
QMSP	Quantitative methylation-specific PCR assay analysis
qPCR	Quantitative real-time PCR
ROIT	Regulator of insulin transcription
WAT	White adipose tissue

Electronic supplementary material The online version of this article (https://doi.org/10.1007/s00125-020-05090-y) contains peer-reviewed but unedited supplementary material, which is available to authorised users.

✉ Liang Jin
ljstemcell@cpu.edu.cn

[1] State Key Laboratory of Natural Medicines, Jiangsu Key Laboratory of Druggability of Biopharmaceuticals, School of Life Science and Technology, China Pharmaceutical University, 24 Tongjiaxiang Avenue, Nanjing, Jiangsu, People's Republic of China

[2] Department of Endocrinology, Nanjing Jinling Hospital, 305 Zhongshan East Road, Nanjing, People's Republic of China

[3] Department of Endocrinology, School of Medicine, Zhongda Hospital, Southeast University, Nanjing, People's Republic of China

Research in context

What is already known about this subject?

- The pancreatic beta cell is solely responsible for the transcription, synthesis and release of insulin and plays a central role in the control of glucose homeostasis
- Abnormal expression of long non-coding RNAs (lncRNAs) has been associated with a variety of human diseases, including diabetes, which play a significant role in beta cell function

What is the key question?

- Are islet lncRNAs involved in obesity-mediated beta cell dysfunction?

What are the new findings?

- The lncRNA ROIT was significantly downregulated in the islets of mice fed a high-fat diet
- Overexpression of ROIT led to improved glucose homeostasis and insulin transcription by binding to DNA methyltransferase 3a and causing its degradation through the ubiquitin proteasome pathway

How might this impact on clinical practice in the foreseeable future?

- These findings functionally suggest a novel link between obesity and beta cell dysfunction via ROIT

Introduction

The pancreatic beta cell is solely responsible for the transcription, synthesis and release of insulin and plays a central role in the control of glucose homeostasis. Failure of beta cell function appears to underlie virtually all forms of diabetes mellitus [1, 2]. Obesity is thought to increase circulating NEFA levels, and chronic exposure to elevated NEFA is detrimental to pancreatic beta cells, resulting in insulin content reduction, insulin secretion deficiency, and beta cells apoptosis [3–6].

Long non-coding RNAs (lncRNAs) are a newly identified class of endogenous RNA molecules, which are typically longer than 200 nucleotides and on rare occasions can encode a functional short peptide [7]. LncRNAs influence the expression and stability of protein-coding RNAs. They also affect DNA methylation, the chromatin landscape, and subsequent gene silencing or activation [8–10]. Abnormal expression of lncRNAs has been associated with a variety of human diseases, including diabetes [11]. Recent studies have identified thousands of lncRNAs in human pancreatic beta cells as well as in mouse pancreatic islet cells [12, 13]. A large proportion of human beta cell lncRNAs is regulated by extracellular concentrations of glucose [14, 15]. We hypothesised that obesity-induced beta cell function failure might be due to alterations in the level of lncRNAs. The aim of this study was to identify islet lncRNAs involved in obesity-mediated beta cell dysfunction via RNA sequence (RNA-seq) analysis and to investigate the mechanism of the regulation of beta cell function by the lncRNA 1810019D21Rik (referred to in this paper as ROIT [regulator of insulin transcription]).

Methods

Animals Five-week-old C57BL/6J mice, *ob*/*ob* mice (8 weeks old), and *db*/*db* mice (8 weeks old) and *db*/- mice, were obtained from the Model Animal Research Center of Nanjing University (Nanjing, China). All animals were on the C57BL/6 background except for *db*/- mice and *db*/*db* mice, which were on the BKS background. C57BL/6J mice were fed a high-fat diet (HFD) for 8 weeks (Catalogue no: D12494, 60% energy from fat, Research Diets, New Brunswick, NJ, USA) using a protocol previously described by Peyot et al [16], and weighed between 40 and 45 g at the end of the 8 weeks on the diet. The control group were fed with a normal diet (Catalogue no: D12450J, 10% energy from fat, Research Diets), and weighed between 20 and 25 g. The mice were randomised to receive the high-fat and normal diet and specify the method of randomisation. All care and handling of animals were carried out according to the appropriate international laws and policies (EEC Council Directive 86/609, 1987), and approved by the animal ethics committee of China Pharmaceutical University (Nanjing, China).

RNA-sequencing analysis Total islet RNA (100 islets per group; three NCD groups, three HFD groups) was isolated using the RNeasy kit (Qiagen, Hilden, Germany). The quality of the samples was assessed and the experiment and data analysis were carried out by Vazyme (Nanjing, China). Cuffdiff (v2.2.1) [17] was used to calculate the fragments per kilobase million (FPKM) for lncRNAs in each group. A difference in gene expression with a p value of ≤ 0.05 was considered significant. The raw data are displayed in Electronic supplementary material (ESM) Table 1. See ESM Methods for further details.

Serum samples of normal-weight and overweight individuals with type 2 diabetes The serum and clinicopathological data used were collected from the Department of Authority of Nanjing Army Hospital, and Zhongda Hospital Southeast University (Nanjing, China). All the individuals enrolled in this study were obese individuals with type 2 diabetes (BMI ≥25 kg/m^2). The negative control individuals were of normal weight (19≤ BMI <25 kg/m^2) and were free from diabetes. All the participants provided written informed consent, and the experiments were approved by the ethics committees of the respective hospitals. *C. elegans* spiked-in control miRNA with 50 fmol of *cel-miR-39* (Applied Biosystems, Foster City, CA, USA) in a 2.5 μl total volume of water was added to 1 ml of human serum, which is an internal control for miRNA in serum [18]. We then performed the purification procedures following the manufacturer's protocol for the miRNeasy Serum/Plasma Kit (Qiagen). The clinical features of the participants are listed in ESM Table 2.

Islet dispersion and insulin-secreting cells C57BL/6J mouse islets were isolated by collagenase digestion and enriched using a Histopaque (Sigma Aldrich) density gradient as described previously [19, 20]. Isolated islets were gathered and resuspended in KRBH balanced buffer containing 0.2% (wt/vol.) BSA supplemented with 2.5 mmol/l glucose, 10% FBS, 100 IU/ml penicillin, and 100 μg/ml streptomycin at 37°C in a humidified 5% CO2 atmosphere. After equilibrating for 90 min, the islets were counted and seeded into 48 well or 6 well plates for further research.

MIN6 cells (passage 20-25), obtained from X. Han (Nanjing Medical University, Nanjing, China) [21, 22], were maintained in DMEM (Gibco, Burlington, ON, USA) containing 15% FBS (Gibco), 100 units/ml penicillin G sodium, 100 μg/ml streptomycin sulphate, and 50 μmol/l β-mercaptoethanol (Sigma Aldrich, St Louis, MO, USA) at 37°C in a humidified 5% CO_2 atmosphere.

To study the effect of palmitate, high glucose and proinflammatory cytokine treatment, islets and MIN6 cells were incubated in 0.5 mmol/l palmitate (Sigma Aldrich), 33.3 mmol/l glucose (Sangon Biotech, Shanghai, China) or a combination of IL-1β (5 ng/ml, Sigma Aldrich) and TNF-α (30 ng/ml, Sigma Aldrich) for 48 h.

Glucose-stimulated insulin secretion (GSIS) assays of the islets and MIN6 cells were performed as described previously [23]. Immediately after incubation an aliquot of the medium was removed for analysis of insulin secretion, and the islets or MIN6 cells were incubated in acid-ethanol for insulin content determination via mice insulin ELISA kit (ExCell Bio, Shanghai, China), and the amount of insulin secretion was normalised by the insulin content. See ESM Methods for further details.

Co-immunoprecipitation MIN6 cells were transfected with pcDNA3.1 and HA-Ub construct or *Roit* overexpression vector and HA-Ub construct for 48 h, and then treated with MG132 (20 μmol/l, MCE, Monmouth Junction, USA) for 6 h. Then IP lysis/wash buffer containing protein inhibitor cocktail was employed to collect protein lysates, which were then centrifuged and incubated with 10 μl of anti-HA immunomagnetic beads overnight at 4°C. To identify binding proteins, the beads were washed and eluted for western blotting.

Subcellular fractionation Cytoplasmic and nuclear RNA was isolated from MIN6 cells using the PARIS Kit (PARI Kit, Invitrogen, Vilnius, Lithuania) according to the manufacturer's instructions. See ESM Methods for further details.

Plasmid construction The *Roit* promoter plasmids, upstream 2 kb (sequence from UCSC, http://genome.ucsc.edu/) of mouse *Roit* was inserted into pGL3-basic vector (Addgene, Watertown, MA, USA). The coding sequences of *Roit*, *Nkx6.1* and *Hnf1b* were amplified by PCR from the full-length cDNA of mice, and then cloned in the pcDNA 3.1 vector to construct *Roit*, *Nkx6.1* and *Hnf1b* expression plasmids (denoted as over-*Roit*, over-*Nkx6.1* and over-*Hnf1b*, respectively).

Dual-luciferase assay *Roit* promoter plasmids or *Roit* promoter mutant plasmids, transcription factors and *Renilla* luciferase were transfected into MIN6 cells. After incubation for 48 h, the luciferase report experiment was performed using the Dual-Luciferase Reporter Assay system (Beyotime, Shanghai, China) to assess the DNA binding and promoter inhibition effect of ROIT.

Chromatin immunoprecipitation The chromatin immunoprecipitation (ChIP) assays were performed using a Magna ChIP A/G kit (Millipore, Billerica MA, USA). Chromatin was immunoprecipitated with anti-HNF1B (1:100 dilution, Novus) and analysed by PCR. The sequences of the primers used for ChIP-PCR are listed in ESM Table 3.

Electrophoretic mobility shift assay analysis The probes were biotin end-labelled (Thermo Scientific Pierce, MA, USA) and then annealed to double-stranded probe DNA. HNF1 homeobox B (HNF1B)–DNA complexes were performed according to the instructions provided with the LightShift Chemiluminescent EMSA kit (Thermo Scientific Pierce, MA, USA). The sequences of the probes are listed in ESM Table 3.

Bisulphite sequencing and quantitative methylation-specific PCR assay analysis DNA was subjected to sodium bisulphite modification using the Methylamp One-step DNA Modification kit (EpiGentek Group, Farmingdale, NY, USA) following the manufacturer's instructions.

For quantitative methylation-specific PCR assay analysis (QMSP), the primers (ESM Table 3) were predicted using the

MethPrimer website (www.urogene.org/cgi-bin/methprimer/methprimer.cgi). The albumin gene (*Alb*) was used as a loading control for all QMSP normalisation. See ESM Methods.

RNA pull-down In vitro transcription of *Roit* was performed with primers containing the T7 promoter sequence (ESM Table 3). RNA pull-down assay was performed according to the manufacturer's instructions (Catalogue no. 20164, Thermo Fisher Scientific, Rockford, MA, USA). See ESM Methods.

RNA immunoprecipitation (RIP) RIP experiments were performed using the Magna RIP RNA-Binding Protein Immunoprecipitation kit (Catalogue no. 17–700, Millipore, Billerica MA, USA). See ESM Methods for further details.

Transfection of lncRNA smart silencer *Roit* smart silencer (si*Roit*123), a mixture of three antisense oligonucleotides (si-1, si-2 and si-3), was synthesised by RiboBio (Guangzhou, China). The target sequences are listed in ESM Table 4. si*Roit*123 or individual si-3 (herein referred to as si*Roit*) was transfected into MIN6 cells and islets via lipofectamine 2000 (Invitrogen, Carlsbad, CA, USA) according to the manufacturer's instructions.

RNA extraction and quantitative real-time PCR analyses Total RNA was extracted from tissues (30 mg tissue per group, 100 islets per group), and cultured cells as described [24]. The primers used are listed in ESM Table 5. Results were normalised to the expression of *Gapdh* and fold of reference genes were calculated by $2^{-\Delta\Delta C_t}$.

Western blot Western blotting was performed as described previously [25]. Results were normalised to glyceraldehyde-3-phosphate dehydrogenase (GAPDH). The antibodies used are listed in ESM Table 6.

Cell Counting Kit-8 assay MIN6 cells were seeded in a 96-well plate (4×10^4 cells/well) in 100 μl culture medium, then the Cell Counting Kit-8 (CCK-8) assay (Vazyme) was performed 0, 24, 48 and 72 h after transfection according to the manufacturer's instructions.

Flow cytometry Forty eight hours after transfection, MIN6 cells were treated with trypsin without EDTA, and the Annexin V-FITC Apoptosis Detection Kit (KeyGen Biotech, Nanjing, China) was used for the detection of cell apoptosis according to the manufacturer's instructions.

In vivo experiments Male C57BL/6J mice (8 weeks old, about 22 g) were randomly divided into five groups ($n = 7$ mice per group). Then, 50, 100, 200 μg si*Roit* dissolved in 0.2 ml normal saline (154 mmol/l NaCl) was injected intravenously into each mouse through the tail vein daily for 3 days. Scrambled siRNA was used as a negative control (siNC), and normal saline as a mock. See ESM Methods for further details.

Immunofluorescence An immunofluorescence assay was performed as described previously [26]. Anti-insulin (1:500 dilution; Novus) and anti-NKX6.1 (1:250 dilution; CST) antibodies were used. Fluorescent images were observed with confocal laser scanning microscope (CLSM, LSM700, Zeiss, Germany).

IPGTT and GSIS in vivo The IPGTT and GSIS tests were performed as previously described [27]. See ESM Methods for further details.

Statistical analysis Student's *t* test was used to assess differences between two groups, and ANOVA was used for multi-group difference analysis. The level of significance was set at $p < 0.05$. Correlations between ROIT expression and the BMI of individuals were performed by linear regression. Data are expressed as mean ± SD or ± SEM. GraphPad Prism 7 software (GraphPad, San Diego, CA, USA) was used for all calculations.

Results

ROIT is downregulated in the islets of obese mouse models To identify the lncRNAs affected by changes in metabolism, and potentially contributing to the development of obesity-associated type 2 diabetes, we performed RNA-seq analysis on RNA isolated from islets of HFD-induced obese mice and mice fed a normal chow diet (NCD). ESM Fig. 1a–d gives information on the weight and blood glucose of the HFD and NCD mice, and the results of the IPGTT. The reads mapped to the mouse genome (GRCM38/mm10) were analysed using GEM software (Marc Kennedy, Sheffield, UK). RNA sequencing yielded about 90 million reads per sample, of which about 85% were mapped to the mouse genome, and novel transcripts were classified from known lncRNAs and protein-coding mRNA. A total of 3203 lncRNAs were detected, 571 lncRNAs were known and 2632 lncRNAs were novel (ESM Table 1, ESM Fig. 1e), of which 2763 lncRNAs were detected in both the HFD mice and the NCD mice. The expression of 342 lncRNAs (of the 2763) was significantly changed; the vast majority (89.2%) of which were downregulated in the islets of HFD mice vs NCD mice (Fig. 1a, ESM Fig. 1f). Raw RNA sequencing data are available from the NCBI Gene Expression Omnibus (GEO series accession number GSE139991).

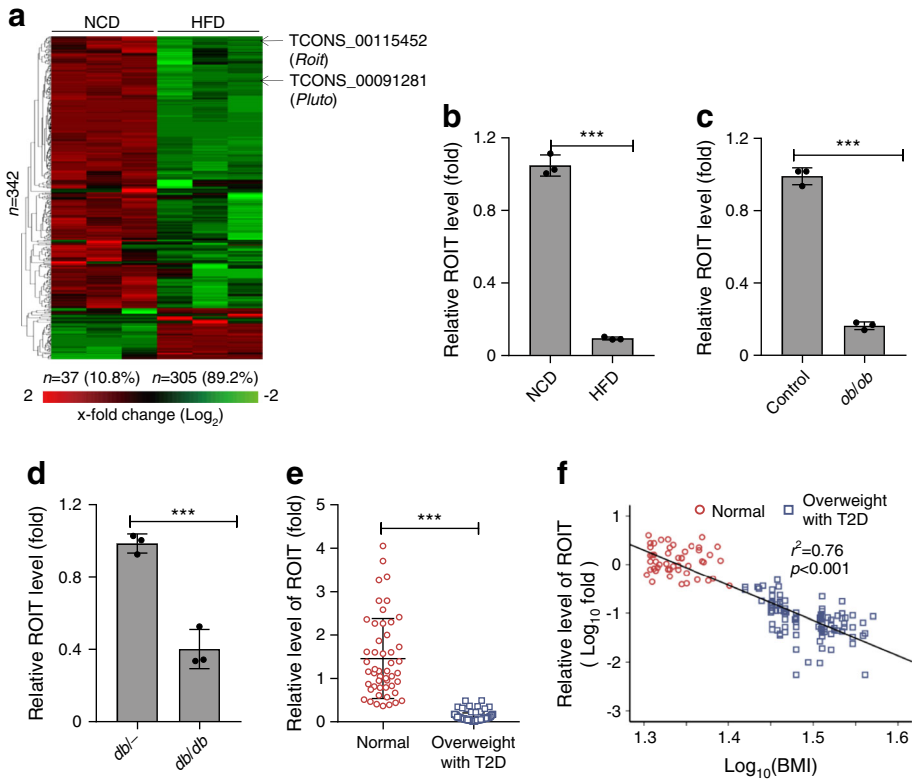

Fig. 1 ROIT expression was downregulated in the islets of obese mice and obese humans. (**a**) Heatmap of differentially expressed lncRNAs in the islets of HFD mice compared with NCD mice. Red and green indicate increased and decreased gene expression levels, respectively. The expression levels of 342 lncRNAs were significantly changed. (**b**–**d**) ROIT was significantly downregulated in the islets of HFD (**b**), *ob*/*ob* (**c**) and *db*/*db* (**d**) mice measured by qPCR ($n = 5$–7). All qPCR experiments were performed in three independent experiments (each independent experiment including $n = 5$–7 mice) each performed in triplicate. Data are mean ± SD. ***$p < 0.001$. Control in part (**c**) is C57BL/6J mice. (**e**) The expression levels of ROIT in the serum pools in normal-weight individuals without type 2 diabetes ($n = 50$; normal) and overweight individuals with type 2 diabetes ($n = 99$; T2D), ***$p < 0.001$, with Ce-miR-39 as positive control (ROIT levels were normalised to Ce-miR-39 before calculating fold). (**f**) Scatter plots of ROIT expression vs BMI. Pearson correlation coefficients (r) and p values were shown. The fold of ROIT was calculated by $2^{-\Delta\Delta C_t}$

The changes observed in the lncRNA levels were confirmed by quantitative real-time (qPCR) analysis of the 20 most dysregulated lncRNAs. More than 90% of the results of qPCR were consistent with those of the RNA-seq analysis, indicating that the results of the RNA-seq were credible (ESM Fig. 1g). This screening confirmed decreased expression of lncRNAs, such as PLUTO, that were previously reported to be associated with diabetes [28] (Fig. 1a). In addition, the decrease in expression was even greater for 1810019D21Rik/ROIT in the islets of HFD mice (Fig. 1a). As shown in Fig. 1b–d, we revealed about nine-, eight- and twofold downregulation of ROIT expression in the islets of HFD-fed mice, *ob*/*ob* mice and *db*/*db* mice, respectively, compared with that in the control. ROIT expression was also decreased in other tissues of HFD mice compared with islets in NCD mice, such as in the liver, white adipose tissue (WAT) and skeletal muscle (ESM Fig. 1h), although to a lesser extent than that observed in the islet. Moreover, we also compared the expression levels of ROIT in the islets and serum of ten HFD mice and NCD mice, revealing that the islets and the serum of these mice shared the same expression pattern of ROIT (ESM Fig. 1i and j). A similar pattern was seen in the ten *db*/*db* mice vs control mice (ESM Fig. 1k and l). Interestingly, ROIT levels were significantly decreased in overweight individuals with type 2 diabetes (BMI ≥25 kg/m^2) compared with those in normal-weight individuals without type 2 diabetes (Fig. 1e), and ROIT expression in the serum correlated significantly with the BMI of these individuals (Fig. 1f). Taken together, our results suggest that ROIT may improve beta cell function during the development of type 2 diabetes.

Characterisation of ROIT The *ROIT* gene is located on chromosome 8 in mice and chromosome 16 in humans (Fig. 2a), which has four annotated transcripts (Fig. 2b). According to previous reports [29], qPCR analyses with primers detecting variants v1-4 or v1+2 revealed that all variants together had about 20-fold higher expression than the long variants v1+2 both in MIN6 cells and islets, suggesting that the short variant v4 represents the major transcript (Fig. 2c). *Roit* was predicted to have no coding potential, and *Roit* transcripts did not reveal any conserved small open reading frames (ORFs) (ESM Fig. 2a).

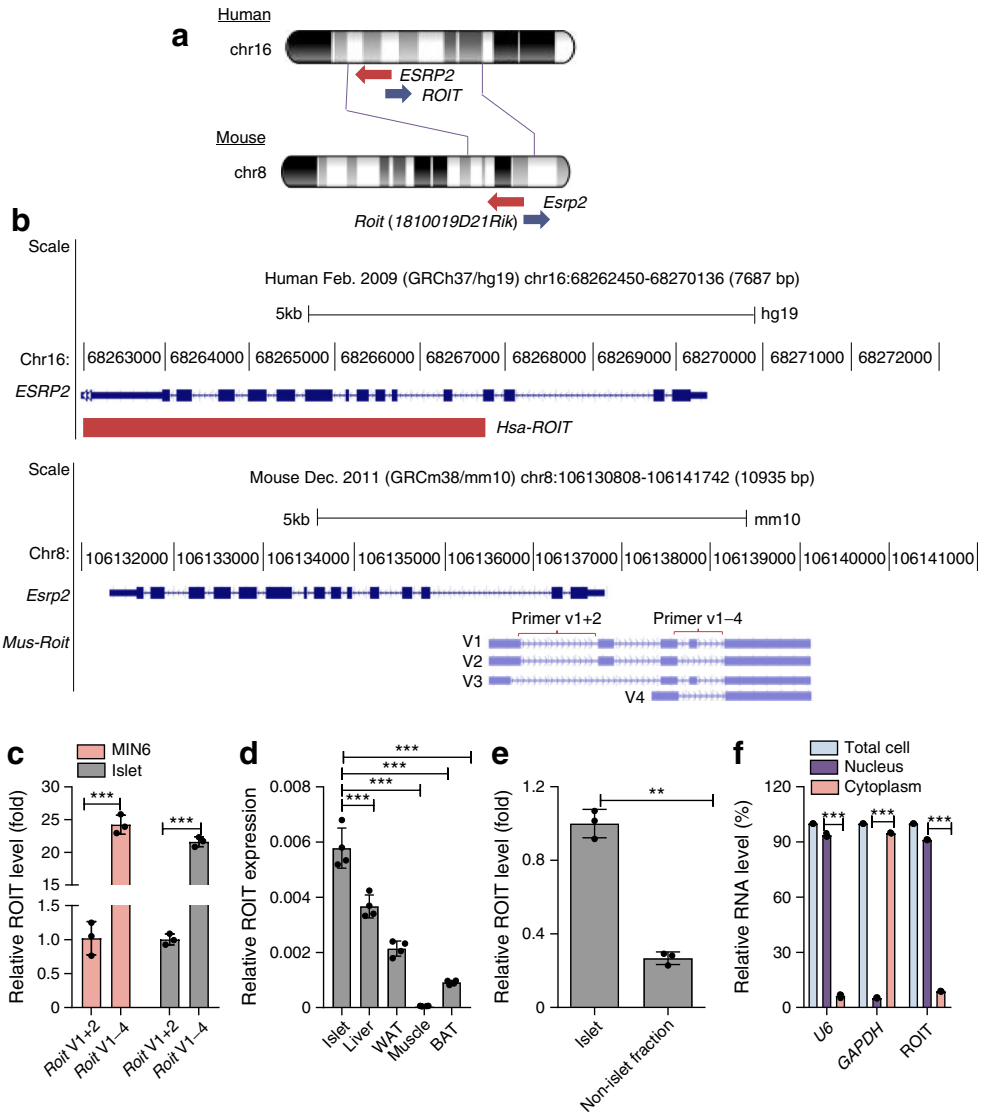

Fig. 2 Characterisation of ROIT. (**a**) *ROIT* is located in a large syntenic block on human chromosome 16 and mouse chromosome 8. (**b**) UCSC Genome Browser scheme of the human *ROIT* (red) and mouse *Roit* variants 1–4 (v1–4, light blue); location of primers detecting *ROIT* v1+2 or v1–4, respectively, is indicated in red. (**c**) qPCR was performed to test the expression levels of ROIT variants 1–4 in MIN6 cell and islets. (**d**) The abundance of ROIT in different tissues of wild-type mice relative to *Gapdh* by qPCR analysis ($n = 4$; $2^{-(\text{ROIT } C_t - \textit{Gapdh } C_t)}$). (**e**) Expression of ROIT in the islet and non-islet fraction ($n = 5$). (**f**) ROIT was enriched in the MIN6 cell nuclear fraction. Levels of ROIT, *Gapdh* mRNA and U6 small nuclear RNA in purified MIN6 cell nuclear and cytoplasm fractions were detected by qPCR. All qPCR experiments were performed in three independent experiments each performed in triplicate. Data are mean ± SD. $^{**}p < 0.01$, $^{***}p < 0.001$. The fold of ROIT was normalised to *Gapdh* mRNA, then calculated by $2^{-\Delta\Delta C_t}$

To assess whether the expression of ROIT is restricted to pancreatic islets, we analysed the level of this lncRNA in a large variety of tissues. We found that ROIT was enriched in islets and was also detectable in muscle, liver, WAT and brown adipose tissue, where the expression was more than ten times lower in muscle than that in the islets (Fig. 2d). Furthermore, we found that ROIT is indeed more abundant in the islet fraction than non-islet fraction (Fig. 2e).

Next, we found that ROIT was mainly distributed in the nuclear fraction of MIN6 cells (Fig. 2f). There is growing evidence that a subset of nuclear lncRNAs functions locally to regulate neighbouring genes [30, 31]. Therefore, we investigated whether ROIT could regulate *Esrp2* (encoding epithelial splicing regulatory protein 2 [ESRP2]) expression, a neighbouring gene of *Roit*. Indeed, we found that knockdown of ROIT resulted in the downregulation of the ESRP2 protein level (ESM Fig. 2b). However, changes in *Esrp2* expression level has no effect on beta cell function (ESM Fig. 2c–e).

Regulation of ROIT expression in the islets of obese mice by HNF1B To determine the possible causes of the changes in ROIT expression detected in the islets of obese mice (HFD, *ob*/*ob* and *db*/*db* mice), we exposed normal mouse islets and MIN6 cells to pathophysiological concentrations of palmitate, glucose and proinflammatory cytokines. The expression of ROIT only decreased in the presence of palmitate (0.5 mmol/l) (Fig. 3a, b, ESM Fig. 3a–d).

Next, we investigated the underlying molecular mechanisms of the downregulated expression of ROIT in the islets of obese mice. Primary islets were exposed to 0.5 mmol/l palmitate for 48 h, and qPCR was performed to confirm the expression levels of high-score transcription factors (score >12.5) of *Roit*, which were predicted by JASPAR (http://jaspar.genereg.net/) and PROMO (http://alggen.lsi.upc.es/cgi-bin/promo_v3/promo/promoinit.cgi?dirDB=TF_8.3) (ESM Table 7). Among these, HNF1B, which has a potential binding site on the *Roit* promoter (ESM Fig. 3e), showed the

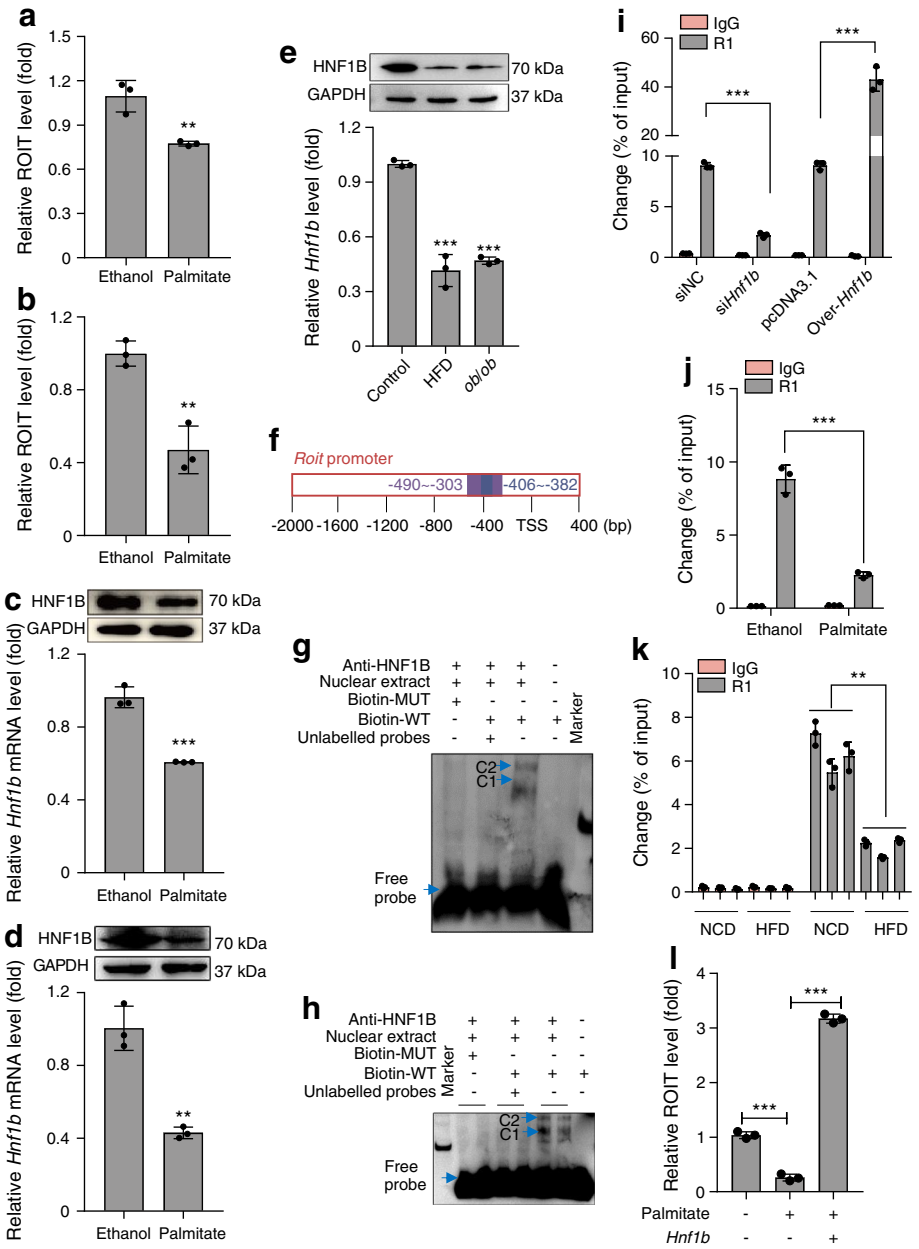

Fig. 3 Knockdown of HNF1B expression results in ROIT downregulation. We used qPCR to examine the expression of ROIT in primary islets (**a**) and in MIN6 cells (**b**) after incubation with 0.5 mmol/l palmitate for 48 h. qPCR and western blotting were performed to measure the expression levels of HNF1B in primary islets (**c**) and in MIN6 cells (**d**) after incubation with 0.5 mmol/l palmitate for 48 h. (**e**) HNF1B expression levels in the islets of obese mice (HFD mice and *ob*/*ob* mice) were assessed by qPCR and western blotting. (**f**) A schematic illustration of the EMSA primer and ChIP primer location. Blue rectangle: EMSA primer location, purple rectangle: ChIP primer location. (**g**, **h**) EMSA analysis revealed that HNF1B could directly bind to the *Roit* promoter in MIN6 cells (**g**) and primary islets (**h**). C1 and C2 represent nuclear protein–*Roit* probe complexes and nuclear protein–*Roit* probe–anti-HNF1B complexes, respectively. Biotin-WT was a 25 bp fragment probe that included the binding region of HNF1B, while Biotin-MUT was a 25 bp fragment probe in which the binding sequence was mutated. (**i**–**k**) The enrichment of HNF1B on the *Roit* promoter relative to IgG detected by ChIP-qPCR assays, in MIN6 cells transfected with over-*Hnf1b*, pcDNA3.1, si*Hnf1b* or siNC (**i**), in MIN6 cells treatment with 0.5 mmol/l palmitate or without palmitate (**j**), and in islets of HFD or NCD mice (**k**, $n = 5$–7). '% of input' indicates the percentage of *Roit* promoter bound by HNF1B compared with input. IgG, negative control; R1, binding site of HNF1B for the *Roit* promoter region. (**l**) ROIT downregulation induced by palmitate was partly reversed by overexpression of *Hnf1b*. All qPCR experiments were performed in three independent experiments, each performed in triplicate. Data are mean ± SD. $^{**}p < 0.01$, $^{***}p < 0.001$ compared with the control. The fold of *Hnf1b* mRNA was normalised to *Gapdh* mRNA, then calculated by $2^{-\Delta\Delta C_t}$

greatest downregulation (ESM Fig. 3f). The mRNA and protein levels of HNF1B were also decreased in primary islets and MIN6 cells (Fig. 3c, d) induced by 0.5 mmol/l palmitate. The same results were observed in obese mice (Fig. 3e).

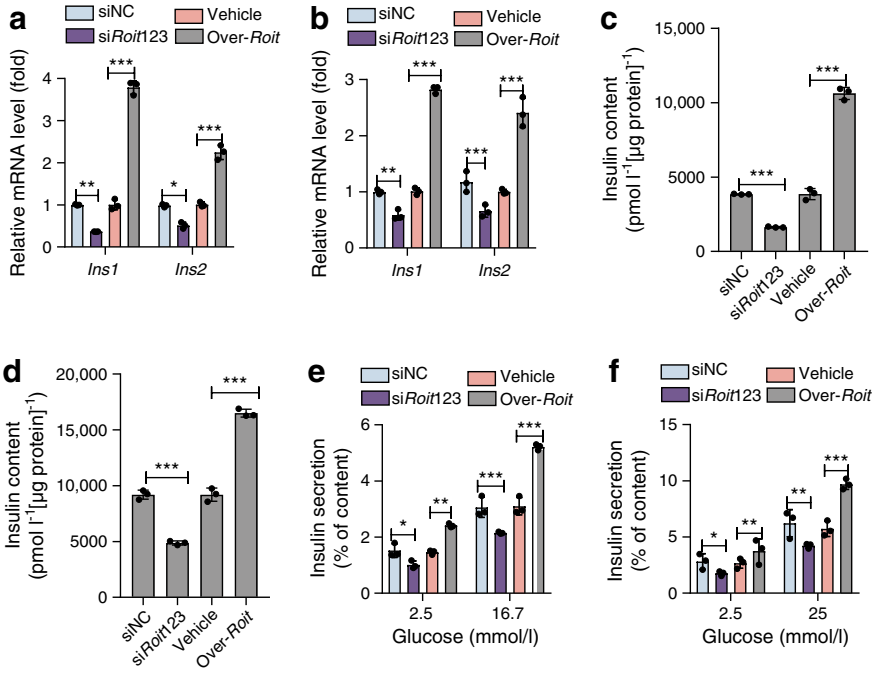

Fig. 4 ROIT inhibition impaired beta cell function in vitro. si*Roit*123 (smart silencer; a mixture of three oligonucleotides: si-1, si-2 and si-3), or over-*Roit* was transfected into primary islets and MIN6 cells for 48 h. qPCR was carried out to determine insulin synthesis in primary islets (**a**) and MIN6 cells (**b**). Insulin content was then tested by ELISA in primary islets (**c**) and MIN6 cells (**d**), and insulin secretion was analysed by a GSIS assay in islets (**e**) and MIN6 cells (**f**). All experiments were performed in three independent experiments, each group contains three batches of individual samples. Data are mean ± SD. $^{*}p < 0.05$, $^{**}p < 0.01$, $^{***}p < 0.001$. The fold of *Ins1 and Ins2* mRNA was normalised to *Gapdh* mRNA, then calculated by $2^{-\Delta\Delta C_t}$

HNF1B is known to be an important regulator of glucose and lipid metabolism [32] and expression of the gene is suppressed by palmitate in islets [33, 34]. We next focused on studying whether obesity facilitates ROIT downregulation by repressing HNF1B expression. We first conducted a dual-luciferase assay and, as expected, this showed overexpression of HNF1B in MIN6 cells (data not shown) and increased transcriptional activity of the *Roit* promoter (ESM Fig. 3g). Next, EMSA assays revealed that the signal from the probe–protein–anti-HNF1B complex was detected using a *Roit* probe in MIN6 cells (Fig. 3f, g); similar results were observed in the isolated islets (Fig. 3h). Furthermore, HNF1B overexpression in MIN6 cells could increase the enrichment of HNF1B in the *Roit* promoter region via a chromatin immunoprecipitation (ChIP) assay (Fig. 3f, i and ESM Fig. 3h). Moreover, we detected that binding of HNF1B to the *Roit* promoter region was decreased in MIN6 cells treated with 0.5 mmol/l palmitate (Fig. 3j, ESM Fig. 3i) and islets isolated from HFD mice (Fig. 3k, ESM Fig. 3j). Further research showed that palmitate-induced ROIT downregulation in islet cells was partly reversed by overexpression of *Hnf1b* (Fig. 3l). Taken together, the results indicate that decreased expression of *Roit* in the islets of obese mouse models is due to the downregulation of expression of HNF1B.

Suppression of ROIT expression decreases insulin synthesis

We next focused on whether ROIT could regulate beta cell function. si*Roit*123 and *Roit* expression plasmid (over-*Roit*) were transfected into primary islets and MIN6 cells for 48 h. The efficiency of knockdown and overexpression were about 70% and 200-fold, respectively (ESM Fig. 4a, b). Over-*Roit* significantly increased the mRNA for the insulin genes (*Ins1* and *Ins2*) (Fig. 4a, b) and the insulin content (Fig. 4c, d), while knockdown induced the opposite result. Glucagon content was not affected by the change in *Roit* levels (ESM Fig. 4c).

Next, we performed a glucose challenge experiments using primary islets and MIN6 cells with knockdown or overexpression of ROIT. Suppression of ROIT expression decreased insulin secretion after exposure to high glucose, and insulin secretion was markedly increased after ROIT overexpression, even at 2.5 mmol/l glucose (Fig. 4e, f). However, ROIT overexpression had no effect on the proliferation or apoptosis of MIN6 cells as assessed by CCK-8 (ESM Fig. 4d), flow cytometry (ESM Fig. 4e) and western blot assays (ESM Fig. 4f, g).

Inactivation of ROIT in normal mice impairs insulin synthesis

To determine the role of *Roit* in regulating insulin synthesis in vivo, we used a smart silencer comprising three independent antisense oligonucleotide sequences (si-1, si-2 and si-3, collectively referred to as si*Roit*123) for the specific knockdown of ROIT. Analysis by qPCR revealed that si-3 was the most effective at knockdown in MIN6 cells, reducing ROIT expression by 70% compared with siNC (Fig. 5a). Thus, the antisense oligonucleotide si-3 (herein referred to as si*Roit*) was used for the subsequent knockdown studies in vivo. We injected si*Roit* intravenously into normal-weight C57BL/6J male mice at three different doses: 50, 100 and 200 μg. Figure 5b shows that a higher suppressive effect on ROIT was observed at the 200 μg dose, resulting in a reduction of almost 60% in the islets compared with that in the siNC group. A decrease in ROIT expression levels in the liver, WAT and skeletal muscle were also observed after injection with 200 μg si*Roit* compared with siNC (ESM Fig. 5a).

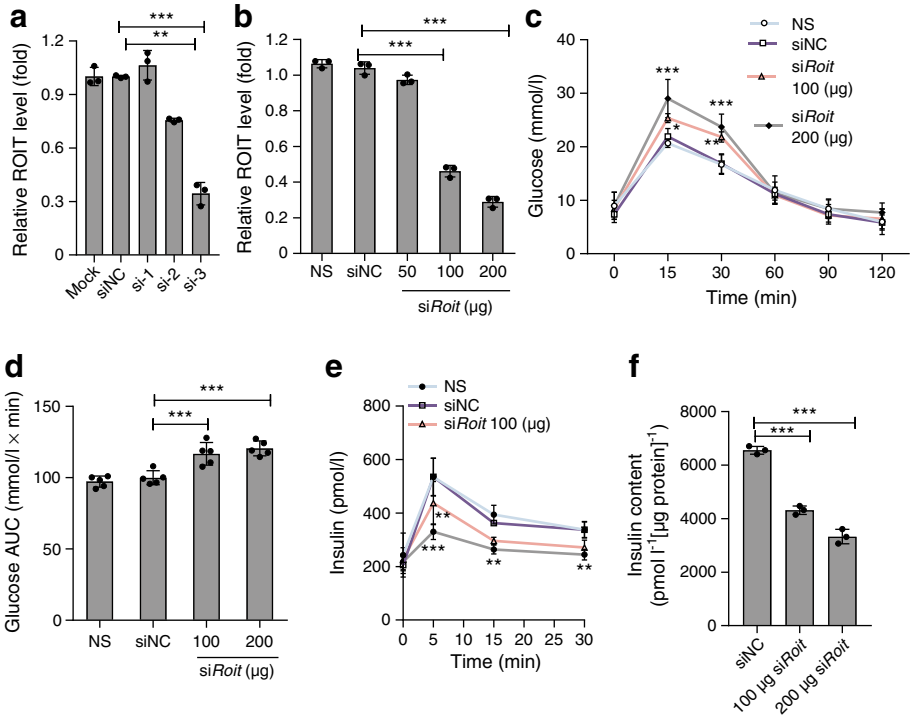

Fig. 5 Inactivation of ROIT impaired beta cell function in vivo. (**a**) MIN6 cells were transfected with smart silencer (a mixture of three oligonucleotides: si-1, si-2 and si-3) targeting ROIT for 48 h, and then qPCR was performed to determine the expression level of ROIT. Because si-3 was the most effective, this was used for subsequent experiments and is referred to as si*Roit* from now on. (**b**) si*Roit* was injected into normal C57BL/6J male mice every day for 3 days. Forty-eight hours after the final injection, qPCR was performed to examine the expression level of ROIT ($n = 3$; pooled samples of islets of Langerhans). (**c**–**e**) IPGTT (**c**), glucose AUC (**d**), and serum insulin levels (**e**) of mice from si*Roit*, siNC and NS (normal saline) groups were detected ($n = 5$ for each group of mice). (**f**) Insulin content was analysed by ELISA ($n = 3$ for each group of mice). In vivo experiments were performed in three independent experiments, each performed in triplicate. Data are mean ± SEM, $^{*}p < 0.05$, $^{**}p < 0.01$, $^{***}p < 0.001$. The fold of ROIT was normalised to *Gapdh* mRNA, then calculated by $2^{-\Delta\Delta C_t}$

In response to an IPGTT, the blood glucose levels in ROIT-silenced mice were elevated in comparison with those in mice from the siNC group, and remained increased for 30 min (Fig. 5c, d). In addition, si*Roit* remarkably decreased the insulin level and insulin content compared with that in the siNC group (Fig. 5e, f), and ROIT silence in vivo has no effect on the levels of the apoptosis markers BCL2 and BCL2-associated X protein (BAX) in the islets (ESM Fig. 5b, c).

***Roit* inhibits transcription of insulin through downregulation of NK6 homeobox 1** To explain how downregulation of ROIT impairs insulin production, we investigated the transcription of the genes for 11 islet transcription factors that play well-established roles in beta cell maturation and insulin transcription using qPCR. Among these, the gene for NK6 homeobox 1 (NKX6.1) was increased most by ROIT overexpression (ESM Fig. 6a). ROIT suppression selectively decreased NKX6.1 both at the mRNA and protein levels (Fig. 6a). Consistent with these findings, islets from the mice i.v. injected with si*Roit* showed decreased *Nkx6.1* mRNA levels, lower levels of staining and protein expression levels of NKX6.1 were observed in the islets from the si*Roit* groups (Fig. 6b, c), which coincided with the impaired expression of insulin.

To explore the role of NKX6.1 in beta cell function, MIN6 cells were transfected with *Nkx6.1*-overexpression plasmid (over-*Nkx6.1*) and si*Nkx6.1*. The ELISA showed that MIN6 cell insulin content and secretion were significantly enhanced by overexpression of *Nkx6.1* (Fig. 6d, e). We then co-transfected islet cells with the *Roit*-overexpression plasmid and si*Nkx6.1* to perform the rescue experiment and found that the upregulation of insulin content and secretion by the *Roit* vector were reversed when co-transfected with si*Nkx6.1* (Fig. 6f, g). A similar result was also observed in MIN6 cells (ESM Fig. 6b, c). Taken together, the results suggest that ROIT can affect islet function by regulating NKX6.1 expression.

ROIT affects the expression of *Nkx6.1* by regulating methylation of its promoter Nuclear lncRNAs are enriched for functionality, involving chromatin interactions, transcriptional regulation, and DNA methylation [35]. To determine whether *Roit* affects the expression of the *Nkx6.1* gene by influencing its methylation, we predicted methylation-sensitive sites in the promoter region of *Nkx6.1* via the MethPrimer website. We found four methylation-sensitive sites in this region (ESM Fig. 7a). We found that the downregulation of Nkx6.1 induced by si*Roit*123 could be reversed by decitabine (DAC, Fig. 7a),

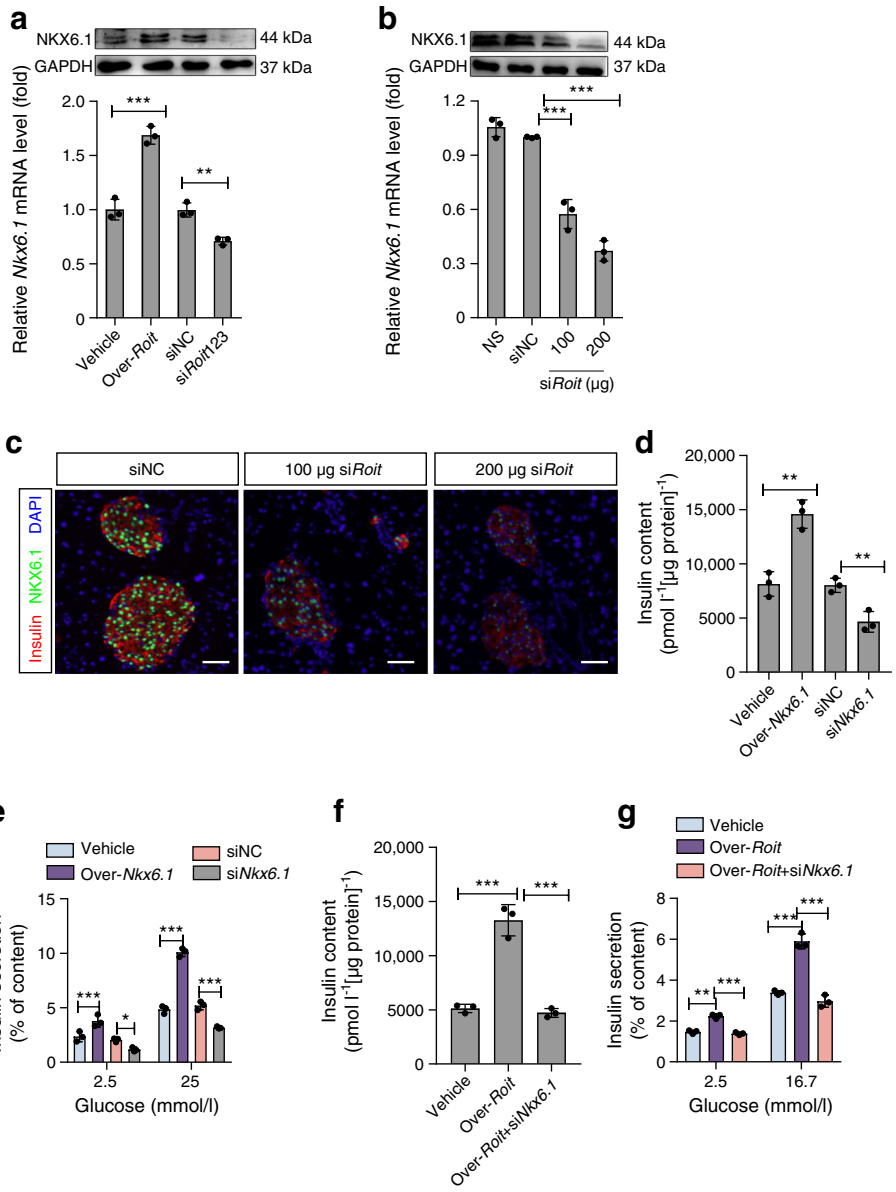

Fig. 6 ROIT affects beta cell function by regulation of NKX6.1 (**a**) si*Roit*123 or over-*Roit* was transfected into MIN6 cells for 48 h, and then qPCR and western blotting were performed to test the expression level of NKX6.1. (**b**) After si*Roit* treatment for 48 h in vivo, qPCR and western blotting were performed to examine the expression levels of NKX6.1 in vivo. (**c**) Double immunostaining was performed for mouse pancreas sections with anti-NKX6.1 (green) in combination with an anti-insulin antibody (red) among three groups. DNA was visualised by staining with DAPI (blue). Scale bar, 100 μm ($n = 3$ per group). (**d**, **e**) si*Nkx6.1* or over-*Nkx6.1* was transfected into MIN6 cells for 48 h and insulin content (**d**) and secretion (**e**) were analysed by ELISA. (**f**, **g**) Primary islets were co-transfected with Over-*Roit* and si*Nkx6.1* for 48 h and then insulin content (**f**) and secretion (**g**) were analysed by ELISA. All experiments described in this figure were performed in three independent experiments, each performed in triplicate. Data are mean ± SD, $^{*}p < 0.05$, $^{**}p < 0.01$, $^{***}p < 0.001$. The fold of *Nkx6.1* mRNA was normalised to *Gapdh* mRNA, then calculated by $2^{-\Delta\Delta C_t}$

which is a DNA methyltransferase inhibitor. This suggested that the expression of *Nkx6.1* was regulated by demethylation.

Next, we measured two distinct regions, named bisulphite sequencing 1 (BSP1) and bisulphite sequencing 2 (BSP2, ESM Fig. 7a). A higher degree (69.7%) of methylation was found in Region 1 in the *Roit* siRNA group than in the *Roit*-overexpressed group (23.4%), and a similar pattern was observed for Region 2 (Fig. 7b). In addition, QMSP analysis revealed that both differentially methylated regions (DMR) of the *Nkx6.1* promoter were found to be more heavily methylated in the si*Roit*123 group (Fig. 7c).

To investigate the effects of the mechanisms of ROIT on the methylation of the *Nkx6.1* promoter, we hypothesised that ROIT might bind to some kinds of proteins that mediate these effects. To identify the protein factors, we first incubated in vitro-transcribed biotinylated ROIT sense or antisense RNA with cell lysate (ESM Fig. 7b–d) and then performed pull-down. The results showed that DNA methyltransferase (DNMT)3A, rather than DNMT1 or DNMT3B, interacted with ROIT (Fig. 7d). Next, RIP assays showed that the DNMT3A antibody instead of the control antibody successfully pulled down ROIT as detected by PCR (ESM Fig. 7e) and qPCR (Fig. 7e). Furthermore, we found that knockdown of ROIT reduced the DNMT3A protein level (Fig. 7f), and the same phenomenon was found when si*Roit* was injected in vivo (Fig. 7g).

To explore the molecular mechanism by which ROIT downregulated DNMT3A expression, we examined the *Dnmt3a* mRNA level in ROIT-overexpressing MIN6 cells. We found that ectopic expression of ROIT did not alter the *Dnmt3a* mRNA level (ESM Fig. 7f), and similar results were observed when si*Roit* was injected in vivo (ESM Fig. 7g). We investigated whether ROIT might reduce the protein level of

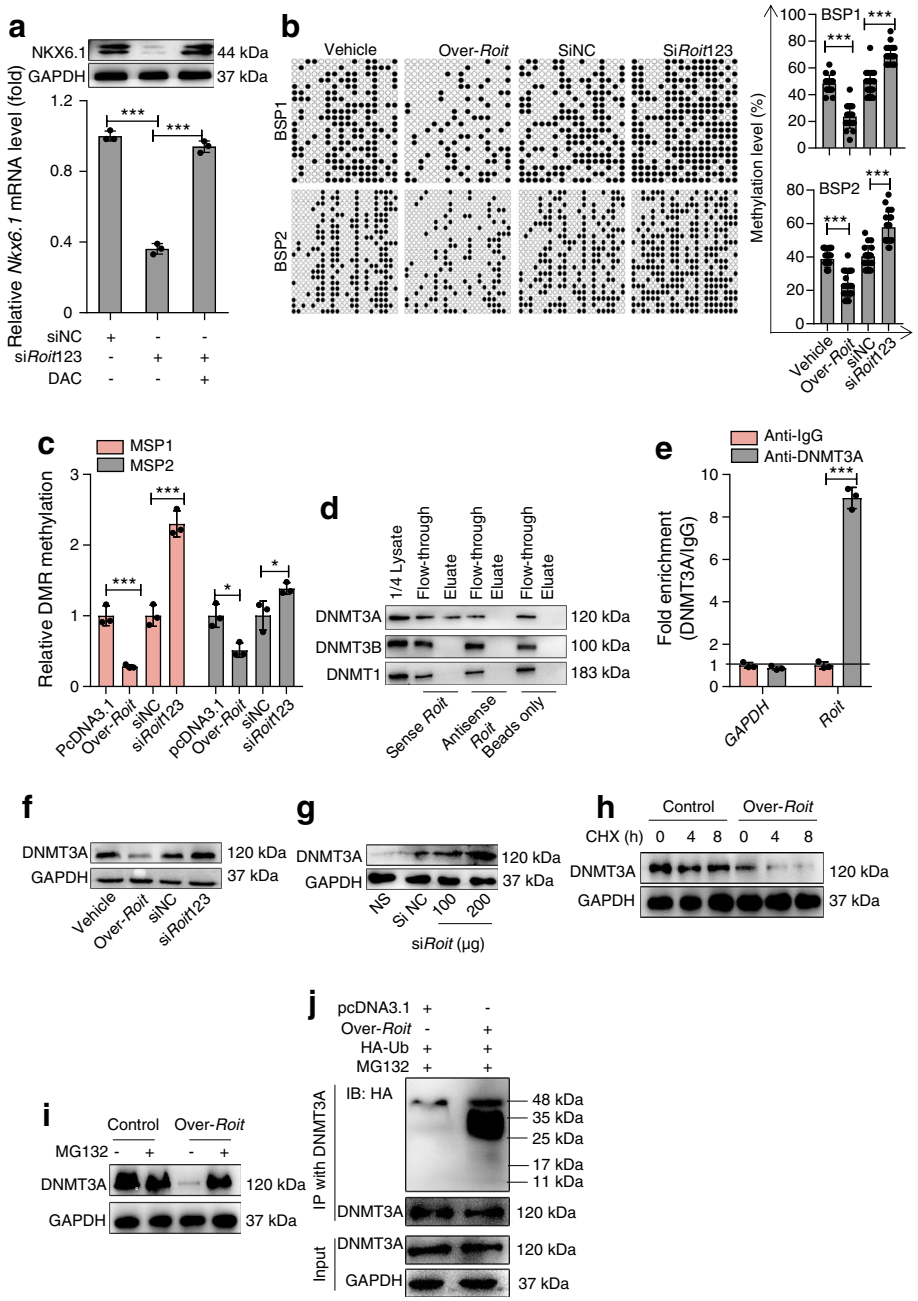

Fig. 7 ROIT promoted insulin synthesis and secretion by binding to DNMT3A and elevating Nkx6.1 expression. (**a**) si*Roit*123 and DAC were co-expressed in MIN6 cells for 48 h, and qPCR and western blotting were performed to examine the expression level of NKX6.1. (**b**) Two BSP regions of the *Nkx6.1* promoter CpG island in MIN6 cells. Each box indicates the methylation status of the CpG site. Each row represents an individual sequenced DNA strand. Over 20 clones from each mixed sample were sequenced. The per cent methylation in each sequenced region is indicated. (**c**) MIN6 cells were isolated 48 h later and analysed using QMSP. (**d**) Western blotting indicated that DNMT3A, rather than DNMT1 or DNMT3B, interacted with ROIT in the pull-down assay. (**e**) The MIN6 cell lysate was subjected to the anti-*DNMT3A* RNA immunoprecipitation (RIP), and the precipitated RNAs were examined by qPCR. *Gapdh* served as a control to validate DNMT3A–*Roit* interaction. (**f**) si*Roit*123 or over-*Roit* was transfected into MIN6 cells for 48 h, and western blotting was performed to test the expression level of DNMT3A. (**g**) The protein expression level of DNMT3A in the islets of mice when injected with si*Roit*. (**h**) MIN6 cells transfected with pcDNA3.1 and over-*Roit* for 48 h, then treated with CHX (20 μg/ml) for 0 h, 4 h and 8 h. Cells were lysed and then subjected to western blotting with the indicated antibodies to monitor the stability of the DNMT3A protein. (**i**) MIN6 cells were transfected with pcDNA3.1 and over-*Roit* for 48 h, and then treated with MG132 (20 μmol/l) for 6 h and subjected to western blotting with indicated antibodies to verify the DNMT3A degradation pathway. (**j**) MIN6 cells were transfected with pcDNA3.1 and HA-Ub construct or over-*Roit* and HA-Ub construct for 48 h, and then treated with MG132 (20 μmol/l) for 6 h. Cells were subjected to immunoprecipitation assay (IP) with anti-DNMT3A antibody followed by immunoblotting (IB) using anti-HA-Tag antibody for detection of DNMT3A ubiquitination. All experiments presented in this figure were performed in three independent experiments, each performed in triplicate. Data are mean ± SD, $*p < 0.05$, $***p < 0.001$ compared with the control. The fold of *Nkx6.1* mRNA was normalised to *Gapdh* mRNA, then calculated by $2^{-\Delta\Delta C_t}$

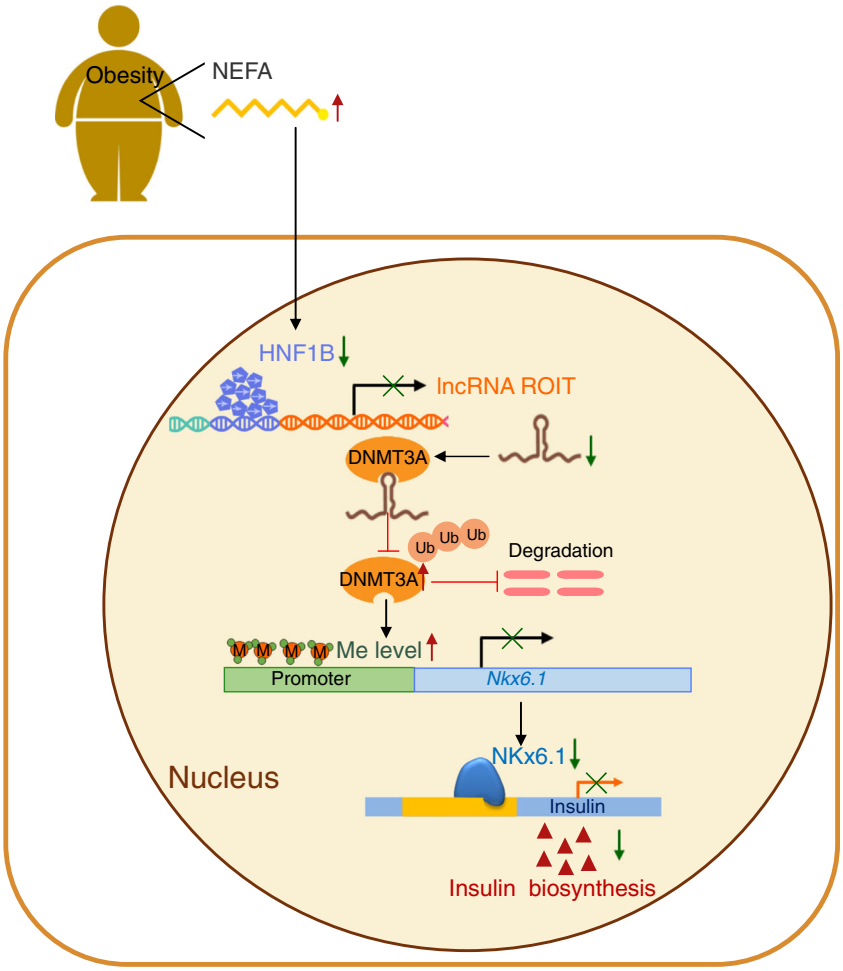

Fig. 8 A working model for the role of ROIT in promoting insulin transcription. During obesity, ROIT is downregulated, suppressing insulin expression and secretion through interaction of ROIT with DNMT3A. DNMT3A protein degradation via the ubiquitin proteasome pathway is inhibited and *Nkx6.1* expression is reduced by methylation of the *Nkx6.1* promoter

DNMT3A by promoting its degradation. DNMT3A degradation was examined in the presence of cycloheximide (CHX), a de novo protein biosynthesis inhibitor. In the presence of CHX, MIN6 cells transfected with over-*Roit* exhibited an increased DNMT3A degradation rate compared with the control group (Fig. 7h). Since the ubiquitin–proteasome pathway is the most ubiquitous pathway for protein degradation, we treated the cells with the ubiquitin–proteasome pathway inhibitor MG132, revealing that MG132 inhibited ROIT induction of DNMT3A degradation (Fig. 7i). Furthermore, we observed increased DNMT3A ubiquitination following ROIT overexpression in MIN6 cells (Fig. 7j). Collectively, these data suggested that overexpression of ROIT could destabilise DNMT3A protein and elevate NKX6.1 gene and protein expression, which improved expression of the insulin genes (*Ins1* and *Ins2*) and insulin secretion.

Discussion

Although obesity is known to cause alterations in the expression of several genes that play important roles in beta cell functions [36], the accurate mechanisms suffering the lipotoxic effects are still a mystery. Herein, we found that ROIT expression was downregulated in the islets of obese mice, which was affected by HNF1B. Decreased ROIT levels inhibited DNMT3A protein degradation and downregulated *Nkx6.1* expression by promoting the methylation of its promoter, which impaired insulin transcription and glucose homeostasis (Fig. 8).

Studies have suggested that conditional NKX6.1 inactivation in adult mice caused beta cell dysfunction and hypoinsulinaemia [37], which can facilitate insulin promoter activation [38] to stimulate insulin synthesis and secretion [39]. In this study we have verified that expression of NKX6.1 is downregulated after knockdown of ROIT. Moreover, the rescue experiment showed that upregulation of insulin content and secretion due to the ROIT vector (over-*Roit*) was reversed when co-transfected with si*Nkx6.1*. Taken together, these results demonstrate that downregulation of ROIT decreased NKX6.1 expression, causing a defect in insulin synthesis and secretion.

Much importance has been attached to the role of DNA methylation in regulating beta cell function in current research

[40–43]. Di Ruscio et al [44] reported that DNMT1 could interact with RNA to block DNA methylation of genes. Our results showed that ROIT decreased the DNMT3A level via direct interaction, which is an important finding based on the fact that the *Nkx6.1* promoter is often modulated by DNA methyltransferases [45, 46]. As expected, our data showed that knockdown of ROIT could increase *Nkx6.1* methylation by upregulation of DNMT3A. To our knowledge, this is the first report of DNMT3A regulation through post-translational modification by ubiquitination. Overall, these results help further understanding of the mechanisms by which ROIT regulates beta cell function. Herein, we found some novel lncRNAs, such as lncRNA-SOX5 and lncRNA-PTPRD by RNA-seq assays, which might play a crucial role in human beta cell function based on previous findings [47, 48]. However, whether these lncRNAs are able to regulate mouse beta cell function is unclear. ROIT lncRNA has been predicted to occur in human beta cells [28], but further study is needed to determine whether ROIT could play a regulatory role in human beta cell function.

In summary, we found that obesity reduced the expression of ROIT through HNF1B. ROIT knockdown inhibited DNMT3A protein degradation and downregulate NKX6.1 expression, which impaired insulin transcription and glucose homeostasis. It suggested that obesity might be relevant to distinct modifications of the expression profile of lncRNAs. An accurate description of the physiopathological conditions caused by disturbances in lncRNA expression will be beneficial to elucidate the causes of beta cell failure and facilitate the design of better tools for diabetes prevention and treatment.

Data availability The datasets generated during the current study are available from the corresponding author upon reasonable request.

Funding This study was supported by the National Natural Science Foundation of China (Grant No. 81570696); the Qing Lan Project; grants from the '111' project (B16046); and the Priority Academic Program Development of Jiangsu Higher Education Institutions (PAPD).

Duality of interest The authors declare that there is no duality of interest associated with this manuscript.

Contribution statement FFZ, YHL, DWW and TSL contributed to the acquisition and analysis of data for this work. FFZ, YY, JMG, YP, YFZ, HD, LL and LJ contributed to the conception and design of the experiments or to the analysis or interpretation of the data for this work. FFZ and LJ wrote the manuscript and all authors made important contributions to editing and revising the manuscript. All authors have approved the final version of the manuscript. LJ is the guarantor of this work.

References

1. Zimmet P, Alberti KG, Shaw J (2001) Global and societal implications of the diabetes epidemic. Nature 414(6865):782–787. https://doi.org/10.1038/414782a
2. Unger RH (1995) Lipotoxicity in the pathogenesis of obesity-dependent NIDDM. Genetic and clinical implications Diabetes 44(8):863–870. https://doi.org/10.2337/diab.44.8.863
3. Cnop M, Hannaert JC, Hoorens A, Eizirik DL, Pipeleers DG (2001) Inverse relationship between cytotoxicity of free fatty acids in pancreatic islet cells and cellular triglyceride accumulation. Diabetes 50(8):1771–1777. https://doi.org/10.2337/diabetes.50.8.1771
4. Maedler K, Oberholzer J, Bucher P, Spinas GA, Donath MY (2003) Monounsaturated fatty acids prevent the deleterious effects of palmitate and high glucose on human pancreatic beta-cell turnover and function. Diabetes 52(3):726–733. https://doi.org/10.2337/diabetes.52.3.726
5. Maedler K, Spinas GA, Dyntar D, Moritz W, Kaiser N, Donath MY (2001) Distinct effects of saturated and monounsaturated fatty acids on beta-cell turnover and function. Diabetes 50(1):69–76. https://doi.org/10.2337/diabetes.50.1.69
6. Butler AE, Janson J, Bonner-Weir S, Ritzel R, Rizza RA, Butler PC (2003) Beta-cell deficit and increased beta-cell apoptosis in humans with type 2 diabetes. Diabetes 52(1):102–110. https://doi.org/10.2337/diabetes.52.1.102
7. Ponting CP, Oliver PL, Reik W (2009) Evolution and functions of long noncoding RNAs. Cell 136(4):629–641. https://doi.org/10.1016/j.cell.2009.02.006
8. Geisler S, Coller J (2013) RNA in unexpected places: long non-coding RNA functions in diverse cellular contexts. Nat Rev Mol Cell Biol 14(11):699–712. https://doi.org/10.1038/nrm3679
9. Pelechano V, Steinmetz LM (2013) Gene regulation by antisense transcription. Nat Rev Genet 14(12):880–893. https://doi.org/10.1038/nrg3594
10. Tsai MC, Manor O, Wan Y et al (2010) Long noncoding RNA as modular scaffold of histone modification complexes. Science 329(5992):689–693. https://doi.org/10.1126/science.1192002
11. Mirza AH, Kaur S, Pociot F (2017) Long non-coding RNAs as novel players in beta cell function and type 1 diabetes. Hum Genomics 11:17
12. Benner C, van der Meulen T, Caceres E, Tigyi K, Donaldson CJ, Huising MO (2014) The transcriptional landscape of mouse beta cells compared to human beta cells reveals notable species differences in long non-coding RNA and protein-coding gene expression. BMC Genomics 15:620
13. Ku GM, Kim H, Vaughn IW et al (2012) Research resource: RNA-Seq reveals unique features of the pancreatic beta-cell transcriptome. Mol Endocrinol 26(10):1783–1792. https://doi.org/10.1210/me.2012-1176
14. Arnes L, Akerman I, Balderes DA, Ferrer J, Sussel L (2016) *βlinc1* encodes a long noncoding RNA that regulates islet beta-cell formation and function. Genes Dev 30(5):502–507. https://doi.org/10.1101/gad.273821.115
15. You L, Wang N, Yin D et al (2016) Downregulation of long noncoding RNA Meg3 affects insulin synthesis and secretion in mouse pancreatic beta cells. J Cell Physiol 231:852–862
16. Peyot ML, Pepin E, Lamontagne J et al (2010) Beta-cell failure in diet-induced obese mice stratified according to body weight gain: secretory dysfunction and altered islet lipid metabolism without steatosis or reduced beta-cell mass. Diabetes 59(9):2178–2187. https://doi.org/10.2337/db09-1452
17. Trapnell C, Hendrickson DG, Sauvageau M, Goff L, Rinn JL, Pachter L (2013) Differential analysis of gene regulation at transcript resolution with RNA-seq. Nat Biotechnol 31(1):46–53. https://doi.org/10.1038/nbt.2450
18. Higuchi C, Nakatsuka A, Eguchi J et al (2015) Identification of circulating miR-101, miR-375 and miR-802 as biomarkers for type 2 diabetes. Metabolism. 64(4):489–497. https://doi.org/10.1016/j.metabol.2014.12.003

19. Gotoh M, Maki T, Satomi S et al (1987) Reproducible high yield of rat islets by stationary in vitro digestion following pancreatic ductal or portal venous collagenase injection. Transplantation 43(5):725–730. https://doi.org/10.1097/00007890-198705000-00024
20. Motterle A, Gattesco S, Caille D, Meda P, Regazzi R (2015) Involvement of long non-coding RNAs in beta cell failure at the onset of type 1 diabetes in NOD mice. Diabetologia 58(8):1827–1835. https://doi.org/10.1007/s00125-015-3641-5
21. Chen F, Sha M, Wang Y et al (2016) Transcription factor Ets-1 links glucotoxicity to pancreatic beta cell dysfunction through inhibiting PDX-1 expression in rodent models. Diabetologia 59(2):316–324. https://doi.org/10.1007/s00125-015-3805-3
22. Lin HY, Yin Y, Zhang JX et al (2012) Identification of direct forkhead box O1 targets involved in palmitate-induced apoptosis in clonal insulin-secreting cells using chromatin immunoprecipitation coupled to DNA selection and ligation. Diabetologia 55(10):2703–2712. https://doi.org/10.1007/s00125-012-2643-9
23. Zhang E, Mohammed Al-Amily I, Mohammed S et al (2019) Preserving insulin secretion in diabetes by inhibiting VDAC1 overexpression and surface translocation in beta cells. Cell Metab 29:64–77.e66
24. Zhu Y, You W, Wang H et al (2013) MicroRNA-24/MODY gene regulatory pathway mediates pancreatic beta-cell dysfunction. Diabetes 62(9):3194–3206. https://doi.org/10.2337/db13-0151
25. Gao H, Zhao Q, Song Z et al (2017) PGLP-1, a novel long-acting dual-function GLP-1 analog, ameliorates streptozotocin-induced hyperglycemia and inhibits body weight loss. FASEB J 31(8):3527–3539. https://doi.org/10.1096/fj.201700002R
26. Tang T, Yang Z, Zhu Q, et al (2018) Up-regulation of miR-210 induced by a hypoxic microenvironment promotes breast cancer stem cells metastasis, proliferation, and self-renewal by targeting E-cadherin. FASEBJ. https://doi.org/10.1096/fj.201801013R
27. Gao H, Song Z, Zhao Q et al (2018) Pharmacological effects of EGLP-1, a novel analog of glucagon-like peptide-1, on carbohydrate and lipid metabolism. Cell Physiol Biochem 48(3):1112–1122. https://doi.org/10.1159/000491978
28. Akerman I, Tu Z, Beucher A et al (2017) Human pancreatic beta cell lncRNAs control cell-specific regulatory networks. Cell Metab 25(2):400–411. https://doi.org/10.1016/j.cmet.2016.11.016
29. Heilmann K, Toth R, Bossmann C, Klimo K, Plass C, Gerhauser C (2017) Genome-wide screen for differentially methylated long noncoding RNAs identifies Esrp2 and lncRNA Esrp2-as regulated by enhancer DNA methylation with prognostic relevance for human breast cancer. Oncogene 36(46):6446–6461. https://doi.org/10.1038/onc.2017.246
30. Sauvageau M, Goff LA, Lodato S et al (2013) Multiple knockout mouse models reveal lincRNAs are required for life and brain development. eLife 2:e01749
31. Vance KW, Sansom SN, Lee S et al (2014) The long non-coding RNA Paupar regulates the expression of both local and distal genes. EMBO J 33:296–311
32. Su S, Wu G, Cheng X et al (2018) Oleanolic acid attenuates PCBs-induced adiposity and insulin resistance via HNF1b-mediated regulation of redox and PPARgamma signaling. Free Radic Biol Med 124:122–134. https://doi.org/10.1016/j.freeradbiomed.2018.06.003
33. Hall E, Volkov P, Dayeh T et al (2014) Effects of palmitate on genome-wide mRNA expression and DNA methylation patterns in human pancreatic islets. BMC Med 12:103
34. Johnstone KA, Diakogiannaki E, Dhayal S, Morgan NG, Harries LW (2011) Dysregulation of Hnf1b gene expression in cultured beta-cells in response to cytotoxic fatty acid. JOP 12(1):6–10
35. Batista PJ, Chang HY (2013) Long noncoding RNAs: cellular address codes in development and disease. Cell 152(6):1298–1307. https://doi.org/10.1016/j.cell.2013.02.012
36. Prentki M, Nolan CJ (2006) Islet beta cell failure in type 2 diabetes. J Clin Invest 116:1802–1812
37. Taylor BL, Liu FF, Sander M (2013) Nkx6.1 is essential for maintaining the functional state of pancreatic beta cells. Cell Rep 4(6):1262–1275. https://doi.org/10.1016/j.celrep.2013.08.010
38. Taylor DG, Babu D, Mirmira RG (2005) The C-terminal domain of the beta cell homeodomain factor Nkx6.1 enhances sequence-selective DNA binding at the insulin promoter. Biochemistry 44(33):11269–11278. https://doi.org/10.1021/bi050821m
39. Schisler JC, Jensen PB, Taylor DG et al (2005) The Nkx6.1 homeodomain transcription factor suppresses glucagon expression and regulates glucose-stimulated insulin secretion in islet beta cells. Proc Natl Acad Sci U S A 102:7297–7302
40. Kaelin WG Jr, McKnight SL (2013) Influence of metabolism on epigenetics and disease. Cell 153(1):56–69. https://doi.org/10.1016/j.cell.2013.03.004
41. Feinberg AP (2007) Phenotypic plasticity and the epigenetics of human disease. Nature 447(7143):433–440. https://doi.org/10.1038/nature05919
42. Dhawan S, Georgia S, Tschen SI, Fan G, Bhushan A (2011) Pancreatic beta cell identity is maintained by DNA methylation-mediated repression of Arx. Dev Cell 20:419–429
43. Dhawan S, Tschen SI, Zeng C et al (2015) DNA methylation directs functional maturation of pancreatic beta cells. J Clin Invest 125(7):2851–2860. https://doi.org/10.1172/JCI79956
44. Di Ruscio A, Ebralidze AK, Benoukraf T et al (2013) DNMT1-interacting RNAs block gene-specific DNA methylation. Nature 503(7476):371–376. https://doi.org/10.1038/nature12598
45. Chang CC, Huang RL, Wang HC, Liao YP, Yu MH, Lai HC (2014) High methylation rate of LMX1A, NKX6-1, PAX1, PTPRR, SOX1, and ZNF582 genes in cervical adenocarcinoma. Int J Gynecol Cancer 24(2):201–209. https://doi.org/10.1097/IGC.0000000000000054
46. Taylor KH, Pena-Hernandez KE, Davis JW et al (2007) Large-scale CpG methylation analysis identifies novel candidate genes and reveals methylation hotspots in acute lymphoblastic leukemia. Cancer Res 67(6):2617–2625. https://doi.org/10.1158/0008-5472.CAN-06-3993
47. Tsai FJ, Yang CF, Chen CC et al (2010) A genome-wide association study identifies susceptibility variants for type 2 diabetes in Han Chinese. PLoS Genet 6:e1000847
48. Axelsson AS, Mahdi T, Nenonen HA et al (2017) Sox5 regulates beta-cell phenotype and is reduced in type 2 diabetes. Nat Commun 8:15652